Molecular conformations and interactions in lurasidone co-amorphous drug systems

DOI: 10.1016/j.molstruc.2021.130709

Joana F. C. Silva Mário T. S. Rosado M. Ermelinda S. Eusébio

Centro de Química de Coimbra, Universidade de Coimbra, R. Larga, 3004-535 Coimbra, Portugal

1. Introduction

Most of the active pharmaceutical ingredients (API) show low aqueous solubility, therefore facing the risk of reduced oral bioavailability and therapeutic efficacy. Co-amorphization is a strategy to enhance their solubility and dissolution rate. However, amorphous phases are metastable, making amorphous drugs prone to crystallization. To overcome stability problems of these metastable phases, recent research approaches have been involving co-amorphous systems of a drug and a small molecule co-former.[1]

This work aims to apply several computational methods to the study of two co-amorphous systems of lurasidone (LUR) with saccharin (SAC) or cysteine (CYS), in order to investigate the local structures and intermolecular interactions responsible for the intimate drug-co-former association that prevents relaxation to the crystalline state.

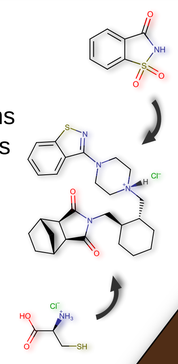

2. Computational methods

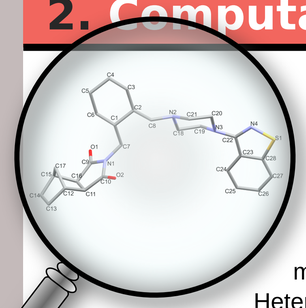

MM+ force field conformational search used relevant torsions and full geometrical optimization with the Hyperchem software. The most frequently obtained molecular geometries were then subject to further complete optimization by DFT using Gaussian 16 software (B3LYP/def2-SVP with GD3BJ dispersion correction).

Selected monomeric and dimeric structures, extracted from the published crystallographic data for LUR,[2] SAC,[3] and CYS,[4] were optimized by the same method.

Heterodimeric geometries were built considering the experimental evidence provided in previously published literature for each co-amorphous system. The electronic structure and intermolecular interactions in the aggregates were analized by two diferent methods: Natural Bond Orbital (NBO),[5] using NBO 6.0, and Non Covalent Interaction (NCI),[6] with NCIPlot4.

3. Lurasidone conformational search

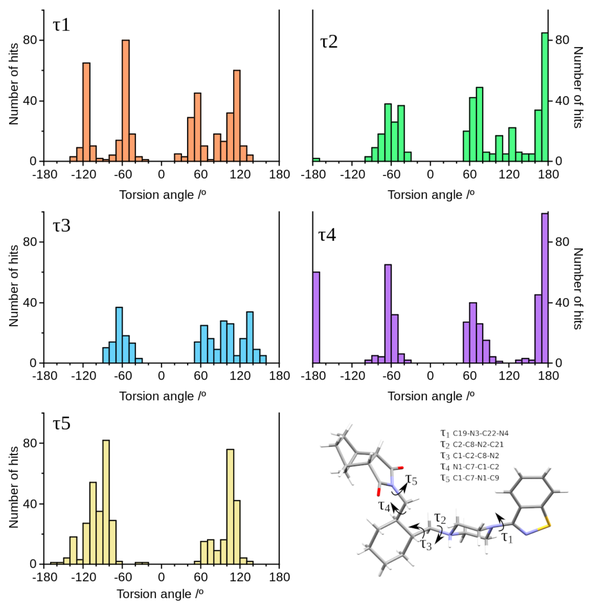

The preliminary MM+ conformational search produced a total of 440 different conformations.

Analysis of the hit frequency of the torsional angles varied in the search shows hints about their most probable values in the conformational space, which are related to the general width of the pits in the potential energy surface.

The resulting structures were used as starting geometries for DFT optimization.

4. DFT geometry optimization: lurasidone

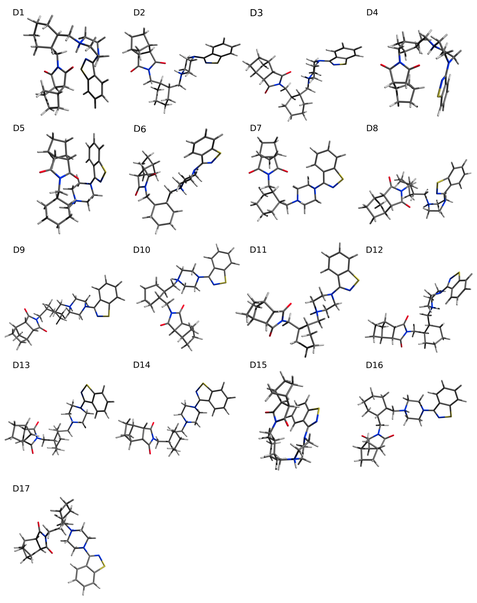

The DFT optimization of the best MM+ and the crystal structures resulted in the 17 geometries in the left.

Torsion values varying upon geometry relaxation of the X-ray crystal monomer shows that τ_1 and τ_2 remain constant, with significant change in τ_4. This means that the benzisothiazole arm remains extended, while the carboximide arm is folded when the structure relaxes.

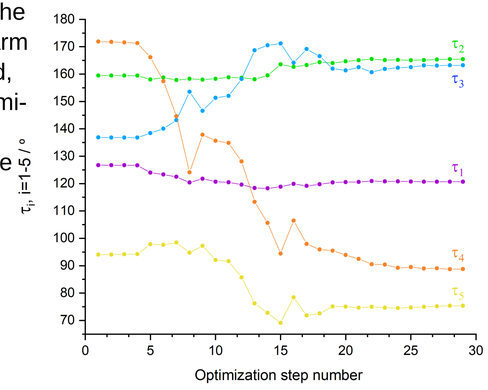

5. DFT geometry optimization: dimers

Analysis of the crystal structure of LUR allowed to establish the dimer as its fundamental supramolecular entity, and it is reasonable to believe that it would be also for the amorphous phase, where short-range order is preserved, nevertheless.

The structure of the homodimer evidences the most important intermolecular interactions as weak H bonds between one of the carboxamide C=O with the HN^+ in the piperazine ring.

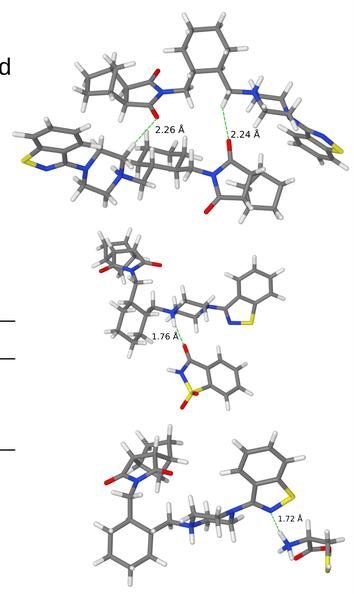

dihedral / °		crystal	B3LYP/def2-SVP homodimer	
			ion 1	ion 2
τ1	N_4-C_{22}-N_3-C_{19}	127	136	118
τ2	C_{21}-N_2-C_8-C_2	160	165	156
τ3	N_2-C_8-C_2-C_1	137	168	167
τ4	C_2-C_1-C_7-N_1	172	−175	173
τ5	C_1-C_7-N_1-C_9	94	95	102

	LUR-SAC	LUR-CYS
X···HN /Å	1.76	1.72
X-H-N /°	164	170
ΔE_{LC} /kJ mol^{-1}	−19.7	−35.8

Heterodimers representing the LUR-SAC and LUR-CYS co-amorphous systems were built from the crystalline structures of each species, manually docked together using the available experimental evidence for their manner of association: LUR-SAC is formed by H bonding, evidenced by FTIR band shifts.[7] The association in LUR-CYS by H bonding was verified by FTIR, Raman, and ss ^{13}C NMR.[8] Heterodimer results show that the lurasidone geometry remains approximately the same as in the crystal, despite establishing strong H bonds with the small co-former molecules. The negative and large values of binding energies confirm their chemical affinity with lurasidone and justify them as a good choice for components of co-amorphous systems.

6. Natural Bond Orbital (NBO) analysis

Within the NBO context, H bonding can be understood as an electron charge transfer from a donor lone pair orbital to an acceptor anti-bonding orbital. Stronger H-bonds have smaller populations in donor and larger in the acceptor orbitals, larger stabilizing 2nd order perturbation energies and, consequently, larger H···Y and smaller X-H bond orders. If the H atom involved in H-bonding is more positively charged, its more acidic character can be also related to a stronger interaction.

In the LUR homodimer, NBO results reveal the weak strength of the H bonding interactions. There are evidently stronger H bonds in the heterodimers. It can be seen as well that the NBO results (bond orders and $E^{(2)}$) indicate that this interaction is stronger in the LUR-CYS heterodimer. This stronger interaction between the unit fragments in the LUR-CYS dimer can be also testified by the larger total charge transfer to the CYS cation than is transferred from the SAC molecule to the LUR cation.

Dimers [a]	**LUR[1]-LUR[2]**		**LUR[1]-SAC[2]**	**LUR[1]-CYS[2]**
Fragment charges [b]	1.007 – 0.993		0.951 – 0.049	1.094 – 0.906
H bond atom charge [c]	0.263	0.261	0.492	0.476
2nd order perturbation analysis [d]	$n(O_2)^1$ ↓ $\sigma^*(H_{18A}C_{18})^2$	$n(O_1)^2$ ↓ $\sigma^*(H_{21A}C_{21})^1$	$n(O_1)^2$ ↓ $\sigma^*(H_{2A}N_2)^1$	$n(N_4)^1$ ↓ $\sigma^*(H_{1A}N_1)^2$
$E^{(2)}$ / kcal mol^{-1} [e]	−2.81	−2.97	−21.27	−37.90
H bonding NBOs occupancy [f]	1.967 ↓ 0.016	1.961 ↓ 0.017	1.935 ↓ 0.065	1.867 ↓ 0.092
Bond orders (NBI) [g] X—H·····Y	0.94 – 0.14	0.94 – 0.10	0.80 – 0.26	0.79 – 0.36

[a] Superscript number in the table identifies the fragment unit in the dimer.
[b] Total charge of each fragment unit.
[c] Charge of H atom involved in H bonding.
[d] Donor NBO → acceptor NBO involved in H bonding. n is a lone pair NBO. σ* is an anti-bonding NBO.
[e] $E^{(2)}$ is the 2nd perturbation energy stabilizing the interaction. superscript number identifies the unit fragment in the dimer.
[f] Occupancy of NBOs in the previous row.
[g] Natural Binding Indices of Natural Cluster Unit analysis.

7. Non-Covalent Interactions (NCI) analysis

Non-Covalent Interactions (NCI) theory provides an index based on the analysis of the electron density **ρ** and its reduced gradient ***s***, or RDG. The electron density can be derived from the SCF wavefunction or from NCI promolecule calculations based on the spacial coordinates, chosen in this work. The 2D plots represent the dependence of RDG from the product of the sign of the 2nd eigenvalue of the electron-density Hessian λ_2 by the electron density, showing weak interaction types and the strength of each interaction.

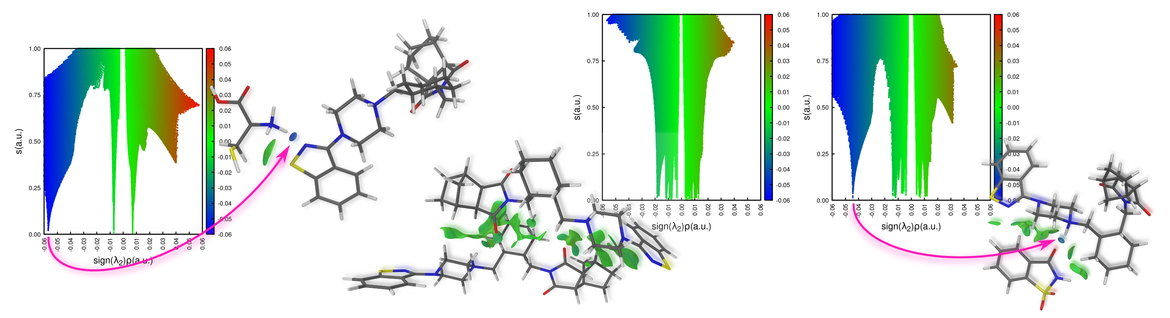

Repulsive interactions — Weak van der Waals interactions — Hydrogen bonding

NCI plots above show the results for the LUR homodimer and the 2 heterodimers. They were restricted to the intermolecular interactions, showing that aggregation in pure LUR is dominated by extensive van der Waals interactions and very weak H bonds (high s in 2D plot). Strong H bonding is visible as blue blobs between the atoms involved in both heterodimers. The analysis of the NCI 2D plots show that the H bond in LURCYS is stronger than in LURSAC, in aggreement with the NBO results.

8. References

[1] Kasten, G.; Löbmann, K.; Grohganz, H.; Rades, T. *Int. J. Pharm.* **2019**, 557, 366–373. https://doi.org/10.1016/j.ijpharm.2018.12.036.

[2] Zhang, H.; Wang, H.; Zhu, X.; Yuan, Z.; Jiang, H. *Acta Crystallogr. Sect. E* **2012**, 68 (5), o1357–o1357. https://doi.org/10.1107/S1600536812012883.

[3] Wardell, J. L.; Low, J. N.; Glidewell, C. *Acta Crystallogr. Sect. E* **2005**, 61 (6), o1944–o1946. https://doi.org/10.1107/S1600536805016600.

[4] Chapman, R. P.; Bryce, D. L. *Phys. Chem. Chem. Phys.* **2007**, 9 (47), 6219–6230. https://doi.org/10.1039/B712688C.

[5] Weinhold, F.; Landis, C. R. "Valency and Bonding: A Natural Bond Orbital Donor-Acceptor Perspective"; Cambridge University Press, 2005.

[6] Contreras-García J, Johnson E R, Keinan S, Chaudret R, Piquemal J P, Beratan D N, Yang W. *J. Chem. Theory. Comput.* **2011**, 7 (3), 625-632. https://doi.org/10.1021/ct100641a.

[7] Qian, S.; Heng, W.; Wei, Y.; Zhang, J.; Gao, Y. *Cryst. Growth Des.* **2015**, 15 (6), 2920–2928. https://doi.org/10.1021/acs.cgd.5b00349.

[8] Heng, W.; Su, M.; Cheng, H.; Shen, P.; Liang, S.; Zhang, L.; Wei, Y.; Gao, Y.; Zhang, J.; Qian, S. *Mol. Pharm.* **2020**, 17 (1), 84–97. https://doi.org/10.1021/acs.molpharmaceut.9b00772.

9. Acknowledgements

JS acknowledges her PhD grant (SFRH/BD/146809/2019) awarded by FCT. CQC is funded by FCT (UIDP/00313/2020)